



Supplement of

Associations of interannual variation in summer tropospheric ozone with the Western Pacific Subtropical High in China from 1999 to 2017

Xiaodong Zhang et al.

Correspondence to: Jianmin Ma (jmma@pku.edu.cn)

The copyright of individual parts of the supplement might differ from the article licence.

SI Text 1. Model evaluation

Extensive model evaluations were performed by comparing simulated ozone concentrations with monitored data collected from China's Environmental Monitoring Center (CNEMC, <http://106.37.208.233:20035/>). The CNEMC started operation in 2013 and provides hourly monitored tropospheric ozone concentrations across China from 2013 onward. Considering large uncertainties of sampled ambient air quality data in the first several years, we collected monitoring data during the summer of 2016-2017 to verify modeled O₃ concentrations. We compared daily modeled and measured O₃ concentrations. **Figure S1a-S1f** show the modeled and sampled daily O₃ concentrations in six UAs during the summer of 2016-2017. The modeled O₃ concentrations capture, to a large extent, the fluctuations of measured concentrations with the correlation coefficients $R > 0.6$ ($p < 0.01$), and even reaches 0.89 in the PRD region. **Figure S1g** is a correlation diagram between the modeled and measured daily O₃ concentrations in six UAs from June 1st, 2016 to August 31st, 2017. Although there are some deviations from the 1:1 line between modeled and measured O₃ concentrations, the fraction of the modeled values is mostly within a factor of two of measured O₃ (FA2) with a correlation coefficient of 0.83 ($p < 0.01$, $n = 1104$).

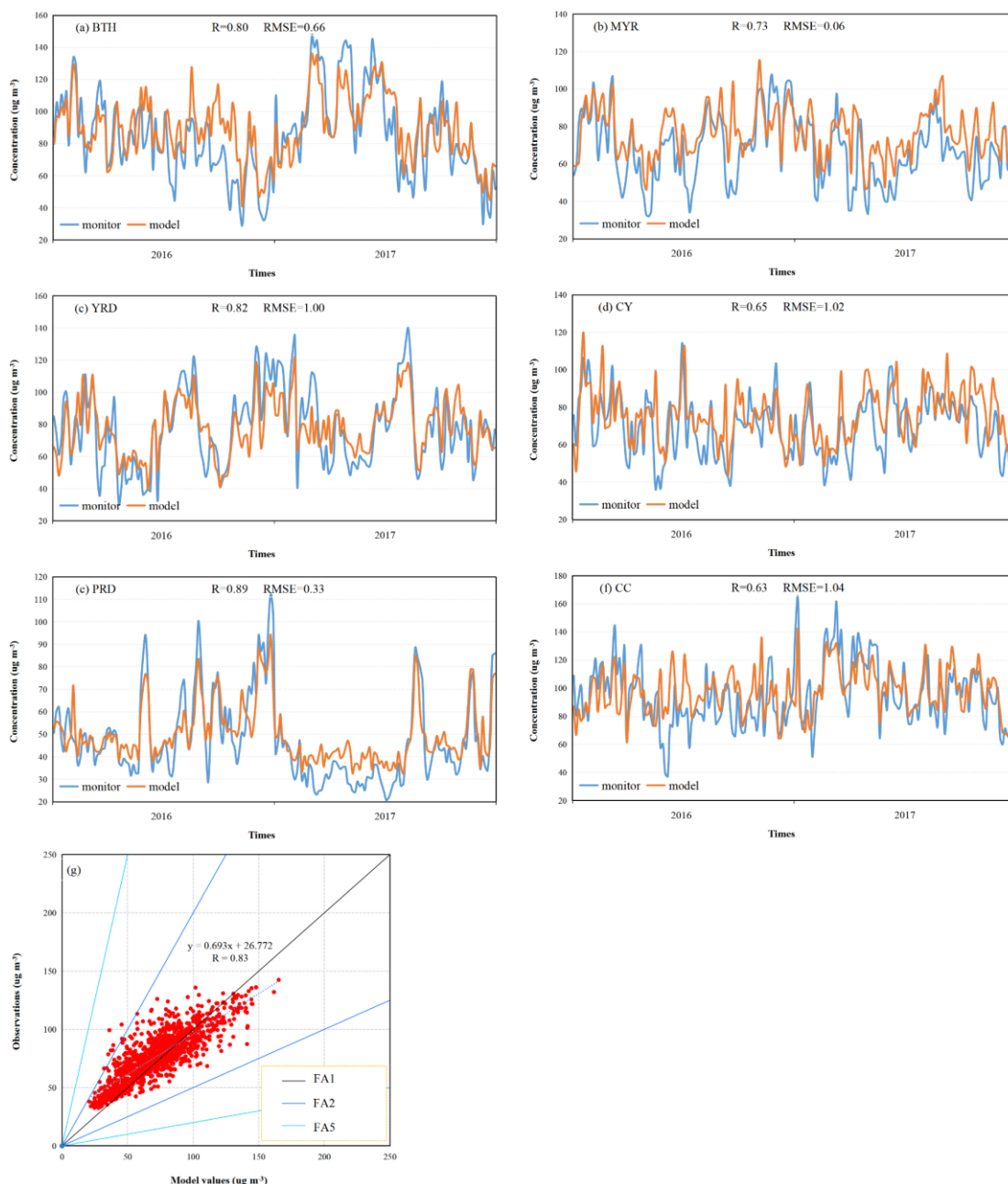


Figure S1. (a-f) Monitored (solid blue line) and modeled (solid orange line) daily O₃ concentrations in six UAs during the summer of 2016-2017. Correlation coefficient (R) and root mean square errors (RMSE) are highlighted in each figure ; (g) A correlation diagram between modeled and measured daily O₃ concentrations in six UAs during 2016-2017 (June, July and August). The number of total samples is 1104. R is correlation coefficient. FA1, FA2, and FA5 are the fractions of model values within factors of one to five of measure O₃ concentrations.

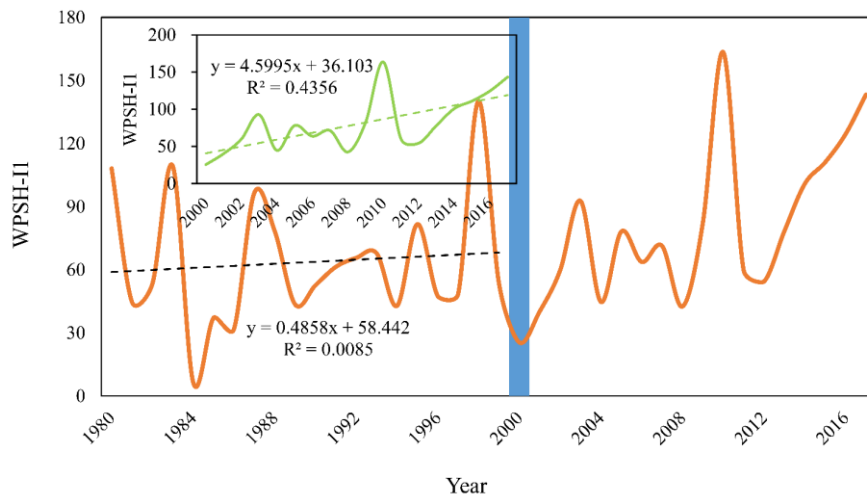


Figure S2. Summer WPSH-I1 from 1980 to 2017. The dashed black line shows the WPSH trend from 1980 to 1999. The inset figure on the top-left shows summer WPSH-I1 from 2000 to 2017 and its trend (dashed green line). Blue shading indicates 2000.

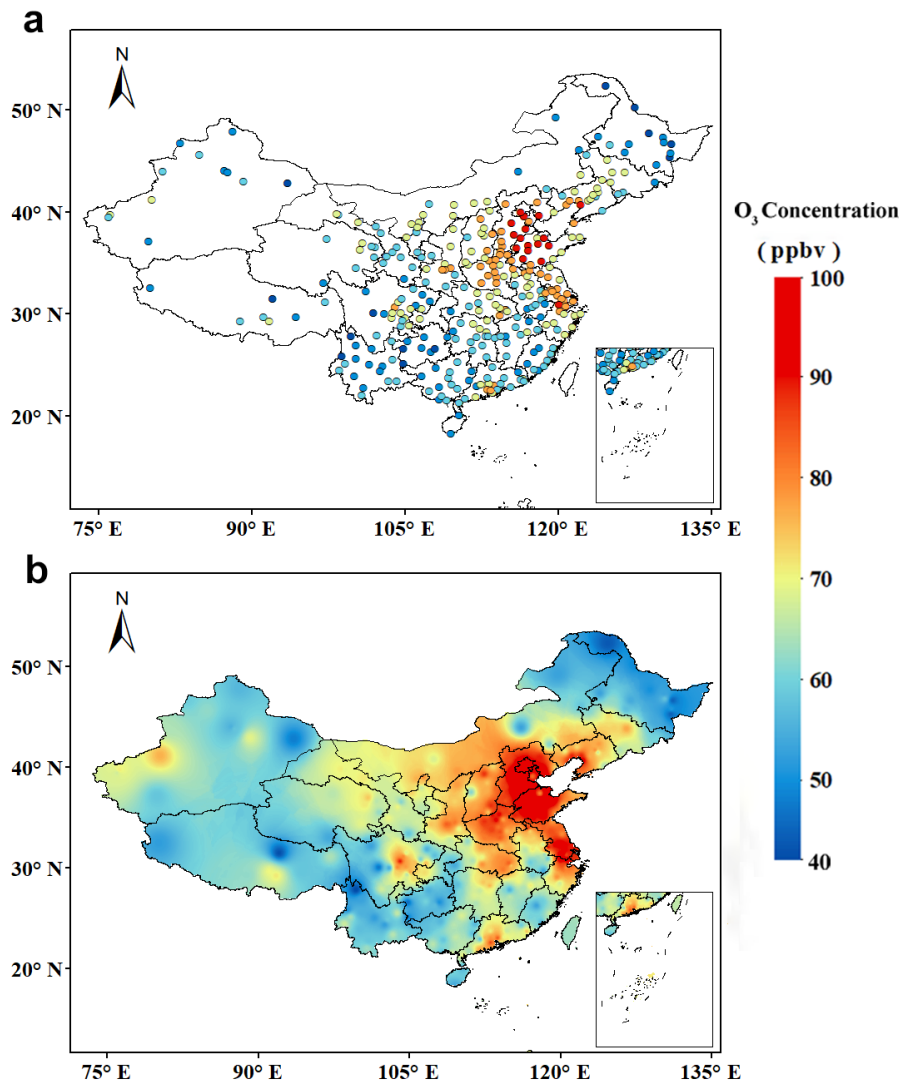


Figure S3. Measured summer O₃ concentrations (ppbv) averaged from 2015 to 2017 across China. (a) Sampled summer O₃ concentrations; (b) interpolated summer O₃ levels.

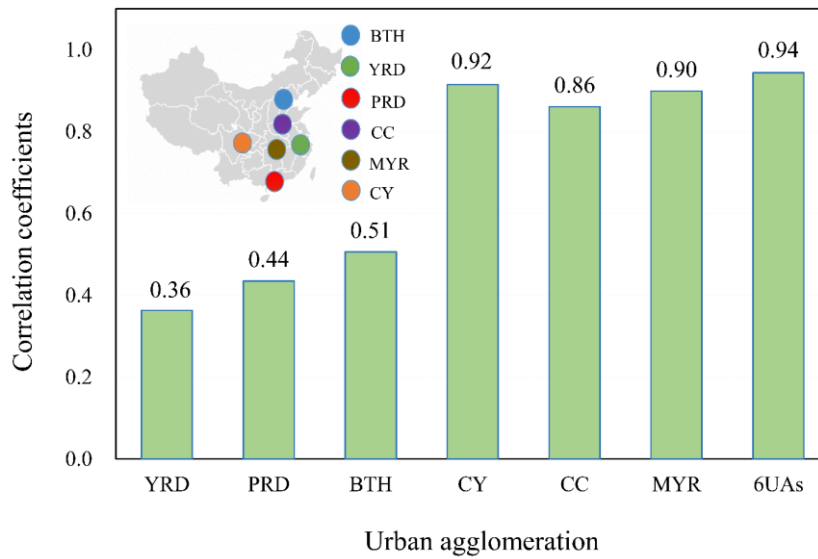


Figure S4. Correlation coefficients between the first EOF loading and summer O₃ concentrations in each UA and averaged over the six UAs from 1999 to 2017. Inner figure on the upper left shows locations of six UAs in China.

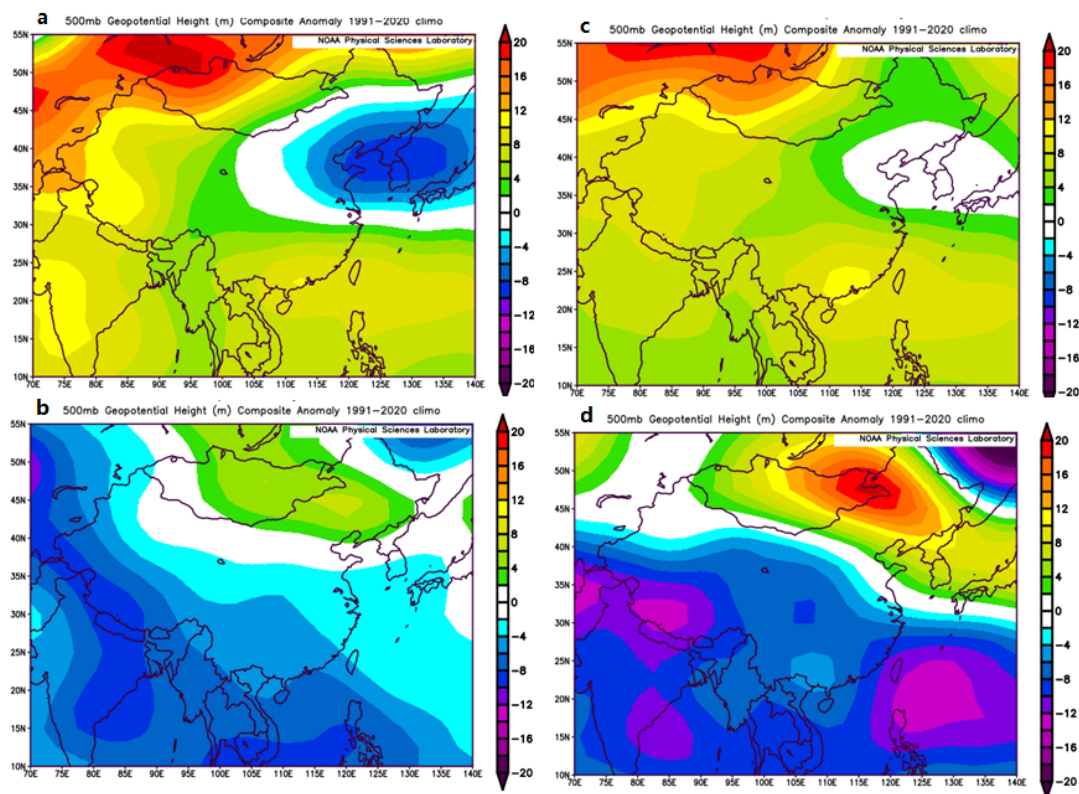


Figure S5. Composite anomalies of 500-hPa geopotential heights (ghm) in positive and negative phases of the first EOF loading (PCA1) for summer O₃ and WPSH-II as the departure from their respective means from 1999 to 2017. We selected those years with the positive and negative anomalies of the PCA1 and WPSHI $\geq \pm 1$ standard deviation. **a.** Composite anomalies in the positive phase of PCA1, **b.** same as

Fig. S5a but for negative phase of PCA1, **c.** composite anomalies in the positive phase of WPSHI, **d.** same as Fig. S5c but for negative phase of WPSHI.

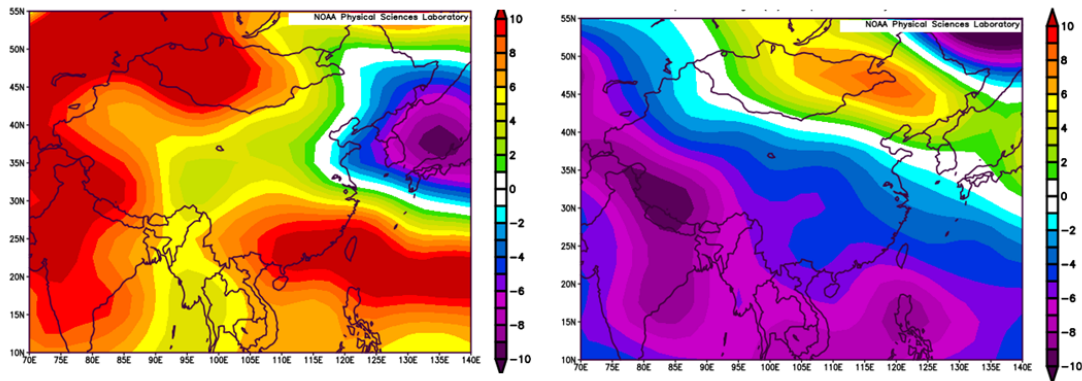


Figure S6. Composite anomalies of 500-hPa geopotential height (ghm) corresponding to **(a)** positive summer O₃ anomalies and **(b)** negative anomalies, estimated by the departure of summer mean O₃ concentrations from their mean averaged from 1999 to 2017. We selected those years with the positive and negative anomalies of O₃ concentrations $\geq \pm 1$ standard deviation (STD, and then estimated their composite means.

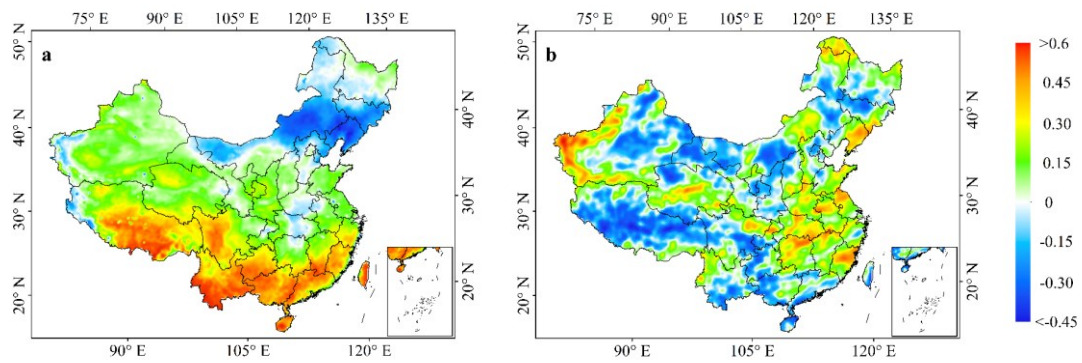


Figure S7. Correlation coefficients between summer WPSH-I1 and SAT **(a)** and precipitation **(b)** simulated under model scenario 2 (S2) from 1999 to 2017.

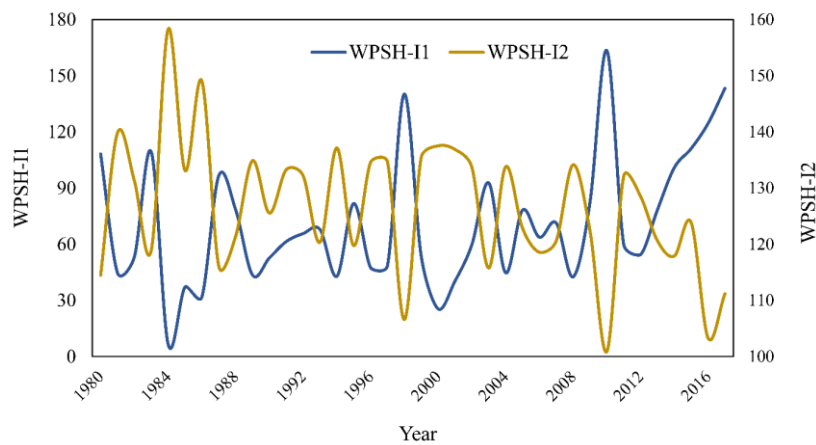


Figure S8. Annual WPSH area index (WPSH-I1) and WPSH ridge point westward shifting (WPSH-I2) from 1980 to 2017.

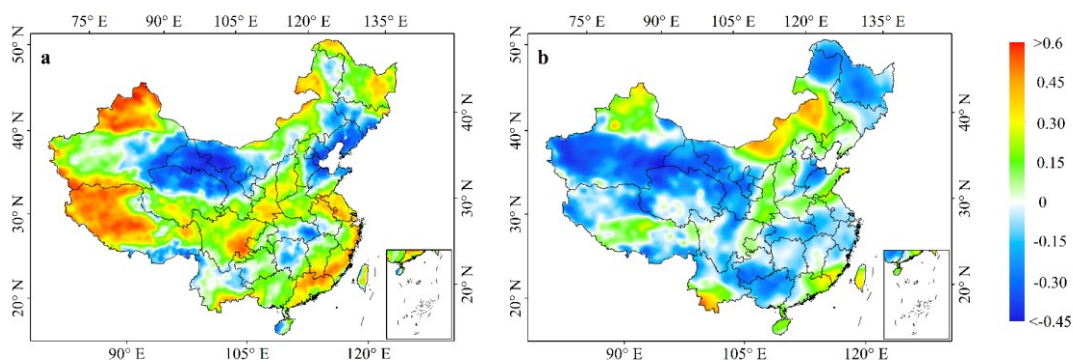


Figure S9. Correlation coefficients between surface incoming solar radiation flux (W m^{-2}) and O_3 concentration (a), and WPSH-I1 (b) from 1999 to 2017.

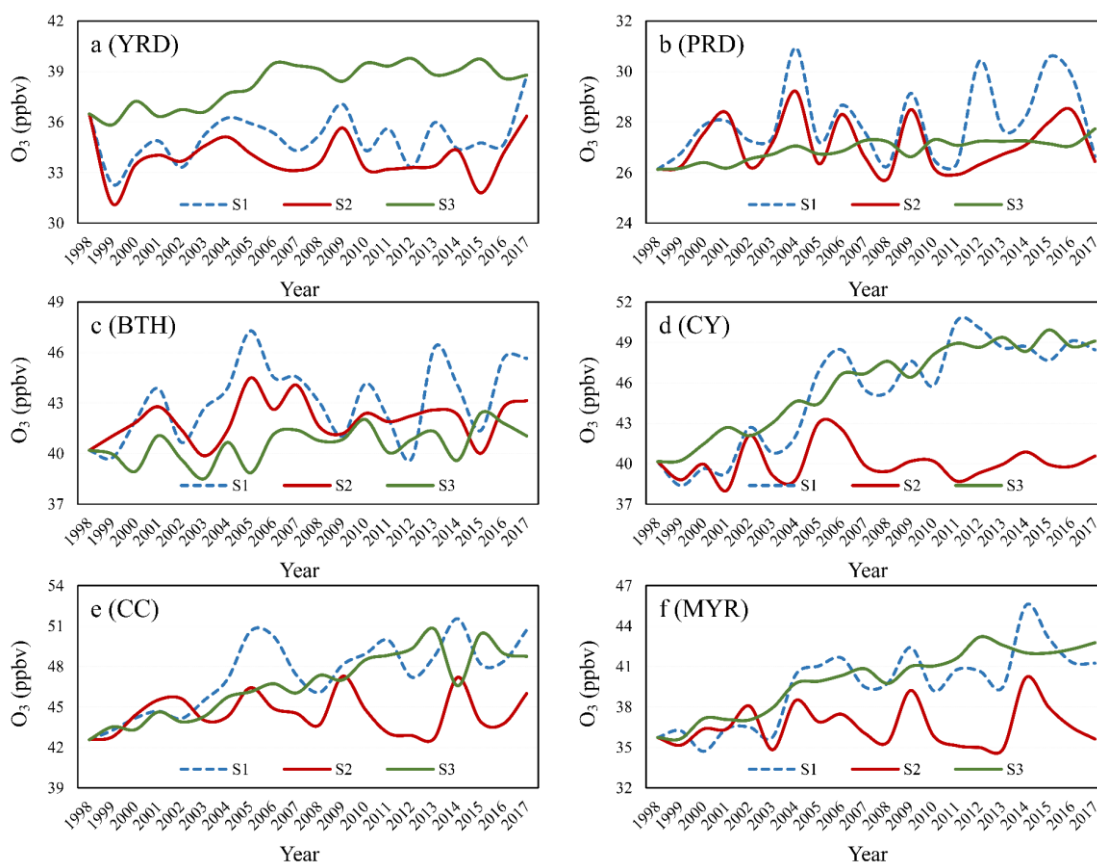


Figure S10. Annual variations of modeled summer O_3 concentrations under three model scenarios averaged over six UAs from 1998 to 2017. (a). summer O_3 concentrations averaged over YRD, S1-S3 indicate three scenarios, (b) same as Fig. S10a but for PRD, (c) same as Fig. S10a but for BTH, (d) same as Fig. S10a but for CY, (e) same as Fig. S10a but for CC, (f) same as Fig. S10a but for MYR.